USGS
science for a changing world

Prepared in cooperation with the U.S. Army Corps of Engineers, Mobile District

Assessing the Impact of Open-Ocean and Back-Barrier Shoreline Change on Dauphin Island, Alabama, at Multiple Time Scales Over the Last 75 Years

By Christopher G. Smith, Joseph W. Long, Rachel E. Henderson, and Paul R. Nelson

Open-File Report 2018–1170

U.S. Department of the Interior
U.S. Geological Survey

U.S. Department of the Interior
RYAN K. ZINKE, Secretary

U.S. Geological Survey
James F. Reilly II, Director

U.S. Geological Survey, Reston, Virginia: 2018

Suggested citation:
Smith, C.G., Long, J.W., Henderson, R.E., and Nelson, P.R., 2018, Assessing the impact of open-ocean and back-barrier shoreline change on Dauphin Island, Alabama, at multiple time scales over the last 75 years: U.S. Geological Survey Open-File Report 2018–1170, 20 p., https://doi.org/10.3133/ofr20181170.

ISSN 2331-1258 (online)

Acknowledgments

This study was funded by the National Fish and Wildlife Foundation through the Gulf Environmental Benefit Fund and in cooperation with study groups of the U.S. Army Corps of Engineers, Mobile District.

Contents

Figures

Tables

Conversion Factors

International System of Units to U.S. customary units

Multiply	By	To obtain
	Length	
millimeter (mm)	0.03937	inch (in.)
meter (m)	3.281	foot (ft)
kilometer (km)	0.6214	mile (mi)
kilometer (km)	0.5400	mile, nautical (nmi)
meter (m)	1.094	yard (yd)
	Area	
square kilometer (km^2)	247.1	acre
square kilometer (km^2)	0.3861	square mile (mi^2)
	Flow rate	
meter per year (m y^{-1})	3.281	foot per year ft y^{-1})
millimeter per year (mm y^{-1})	0.03937	inch per year (in y^{-1})

Datum

Vertical coordinate information is referenced to the North American Vertical Datum of 1988 (NAVD 88).

Elevation, as used in this report, refers to distance above the vertical datum.

Abbreviations

ceDI	composite eastern Dauphin Island
DI	Dauphin Island
Esri	Environmental Systems Research Institute, Inc.
ETD	ebb-tide delta
FTD	flood-tide delta
LDI	Little Dauphin Island
lidar	light detection and ranging
MHW	Mean High Water
seDI	simple eastern Dauphin Island
swDI	simple western Dauphin Island
USACE	U.S. Army Corps of Engineers
USDA	U.S. Department of Agriculture
USGS	U.S. Geological Survey
WDL	Wet Dry Line
WLR	Weighted Linear Regression

Assessing the Impact of Open-Ocean and Back-Barrier Shoreline Change on Dauphin Island, Alabama, at Multiple Time Scales Over the Last 75 Years

By Christopher G. Smith, Joseph W. Long, Rachel E. Henderson, and Paul R. Nelson

Abstract

Dauphin Island and Little Dauphin Island, collectively, make up a geomorphically complex barrier island system located along Alabama's southern coast, separating Mississippi Sound from the Gulf of Mexico and Mobile Bay. The barrier island system provides numerous economical (tourism, fisheries) and natural (habitat for migratory birds, natural protection of inland and coastal areas from storms) benefits to the State of Alabama. The complex geomorphology of Dauphin Island is partly a response to temporal variations in the direction and magnitude of sediment transport along and across the barrier island system. In this report, we present open-ocean and back-barrier shoreline change rates at different time scales to evaluate the island's dominant behavior (expansion or widening and contraction or narrowing) over the last 75 years. The spatial and temporal variability of barrier island width provides baseline and historical context for potential restoration alternatives being considered as part of the Alabama Barrier Island Restoration Feasibility Study. Open-ocean shorelines have eroded continuously over the last 75 years, with rates ranging from 1.5 to 4 meters per year. Back-barrier shorelines are less uniform than open-ocean shorelines, but are, on average, also eroding over the same period. Periods of back-barrier progradation are observed but generally occur during discrete, large altering events like hurricanes that overwash or breach narrow sections of the barrier island. Because both shorelines are eroding, the width of the island has decreased during the last 75 years. The section to the west of a breach that opened during Hurricanes Ivan and Katrina (known as Katrina Cut) exhibits a steady, rapid decrease in width while the section to the east of the breach has gone through periods of expansion and contraction and has only recently begun slowly narrowing. Although the recent trends indicate declining widths, the back-barrier progradation rates in this area were the highest compared to other time periods, which abated extreme narrowing caused by increased open-ocean shoreline erosion. These data and the interpreted results indicate that both short-term (annual) and long-term (decadal) cross-barrier sediment exchange is a key component of sustaining barrier island width. Therefore, any mechanisms that influence this exchange, whether from natural processes (overwash, breaching, or inlet dynamics) or human activities (development, post-storm recovery, restoration), should be considered when evaluating the long-term sustainability of barrier island systems.

Introduction

Barrier islands are dynamic, coastal landforms that provide critical habitat for a number of ecologically and economically important species, serve as natural barriers during elevated wave conditions associated with tropical and extratropical storms, and separate estuaries from

oceans, allowing for additional habitat function. Barrier islands are also high-demand recreational destinations (fishing, beach tourism) and provide significant economic benefits to local, State, and Federal agencies. Finding a balance between the natural and anthropogenic demands on these coastal landforms has been a challenge over the last century as more and more people move to the coast. Thus, the dynamics of barrier islands has increased multifold due to pressures exerted by humans and natural processes on the landform, habitats, and indigenous species.

The Mississippi-Alabama barrier island chain separates Mississippi Sound from the northern Gulf of Mexico. The barrier island chain begins in southwest Alabama, west of Mobile Bay Channel and extends 100+ kilometers (km) to the west. Among this stretch of barrier islands, Dauphin Island, Alabama, is geomorphically unique (fig. 1). The island's uniqueness stems from its three distinct geomorphic regions and their geologic underpinning (Otvos, 1970): (1) a wide region makes up the eastern most one-fifth of the main east-west trending Dauphin Island, (2) a narrow region compromises the western four-fifths of the island, and (3) a secondary barrier island (Little Dauphin Island) lies north of the eastern section of Dauphin Island and trends southeast-northwest.

Barrier island geomorphology can be described as either simple or composite, owing in part to the stratigraphic and geologic (origin) history of the system. Simple barrier islands (and associated barrier platforms) are low and narrow transgressive landforms, bars, or spits dominated by overwash, inlet, and alongshore transport; whereas, composite barrier islands are tall and wide systems with one or more relict or modern progradational feature often underpinned by some antecedent geologic unit (Otvos, 1970; Riggs and others, 1995). The wide, eastern region of Dauphin Island is one such composite barrier island (Otvos, 1970). This section of the island is 5 km alongshore, 0.7–1.2 km wide, and 0–10+ meters (m) above local mean sea level. A Pleistocene-age platform escarped during previous sea-level highstand and fronting Holocene-age strandplains or ridgeplains are the cause of the unique dimensions of the island relative to other Gulf of Mexico barrier islands. This same unit underlies much of Little Dauphin Island as well. The geomorphology of the western region (approximately 19 km alongshore) is narrow (0.2–0.3 km), low (0–3 m), and best described as a simple barrier island. Sediment transport is largely alongshore (east to west); however, cross-shore transport occurs during elevated water levels, and energetic wave conditions occur during storms and at inlets.

Although the underlying geology of Little Dauphin Island is like that of the wide, eastern region of Dauphin Island, interactions between Mobile Pass and Dauphin Island produce an additional layer of geomorphic complexity. Little Dauphin Island lies to the north of Dauphin Island and trends obliquely, northwest to southeast (fig. 1). The modern sand shoreline (northeast side) of Little Dauphin Island is remarkably linear, whereas the back-barrier marsh shoreline is complex with varying marsh platforms, tidal channels, and relict inlet and overwash-related features. The dominant alongshore flow is from northwest to southeast and is influenced by ebb flow through Mobile Pass and northeast wind waves moving across Mobile Bay from late summer to early winter (Hummell, 1999). Thus, although Little Dauphin Island is a barrier island itself, it is geologically linked to Dauphin Island and Mobile Pass (Douglas, 1994).

Pelican Island and Sand Island are related islands south of Dauphin Island (fig. 1). Both islands have an arcuate shape; Pelican Island has a fairly stable trend from northwest to southeast while Sand Island trend varies northeast to southwest through northwest to southeast. These islands have reportedly formed, merged, grown, and disappeared at least once in the last century (Otvos, 1981, 1985; Douglas, 1994; Otvos and Carter, 2008; Byrnes and others, 2010).

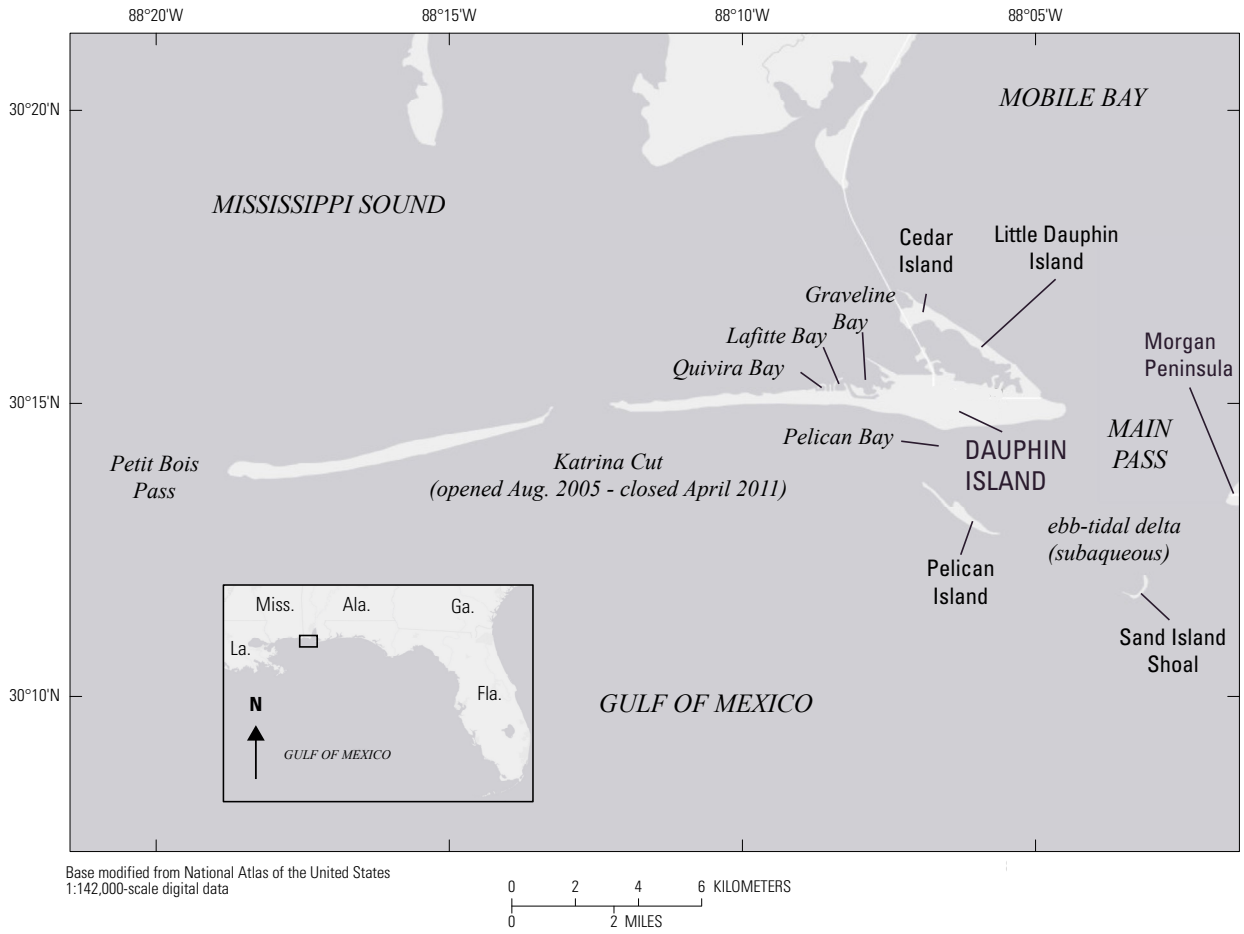

Figure 1. Site map showing specific geographic locations on and surrounding Dauphin Island, Alabama.

In literature concerning northern Gulf of Mexico barrier island systems, Pelican and Sand Island names are used synonymously and separately; however, the latter tends to be the preferred convention. In 2008, Pelican Island merged with Dauphin Island at the point where Dauphin Island transitions from a composite to a simple barrier island.

Dauphin Island (including its undeveloped western end) protects Alabama's mainland coastal communities and resources from storms and provides expansive coastal habitat, with more than 200 acres of beach, dunes, overwash fans, intertidal wetlands, and maritime forest and freshwater ponds in addition to subtidal habitat (Enwright and others, 2017). These habitats support many living coastal and marine resources, including threatened and endangered species such as the piping plover (*Charadrius melodus*). The island also protects the eastern Mississippi Sound ecosystem by modulating the wave energy and preserving the salinity structure for submerged aquatic vegetation as well as oysters, shrimp, crabs, and other species. Extreme events have had a large impact on Dauphin Island over the past decades, including Hurricanes Frederic (1979), Ivan (2004), Katrina (2005), and Isaac (2012) as well as anthropogenic events like the Deepwater Horizon oil spill (2010). Historical efforts have focused on maintaining and restoring the island to pre-event condition. However, a comprehensive plan for restoration of Dauphin Island focusing on its importance to the State's natural coastal resources has not been developed. The goal of the Alabama Barrier Island Restoration Feasibility Study is to develop this comprehensive plan.

One of the leading concerns for much of Dauphin Island is the narrowing of the barrier island west of the Pelican Island–Dauphin Island merger. Numerous studies (for example, Douglas 1994; Morton, 2008; Byrnes and others, 2010) have looked at erosion rates on the island and developed sediment budgets to evaluate potential causal relations with anthropogenic modifications (such as Mobile Bay Channel dredging) and storm events (Hurricanes Frederick, Ivan, Gustav, and others). The current study adds to previous literature by examining potential connections or disconnections between oceanic shoreline change and back-barrier shoreline change as metrics for characterizing changes in barrier island width. For example, the western four-fifths of Dauphin Island not only relies on alongshore sediment transport but also on cross-barrier transport during storms (overwash) to maintain subaerial environments. Thus, we analyzed both oceanic and back-barrier shoreline position data to assess the history of cross-barrier transport by way of (dis)equilibrium in shoreline change rates and width change on the geomorphic evolution of Dauphin Island.

Methods

Shoreline Detection

Shorelines along the ocean and estuarine (back barrier) coasts of Dauphin Island were derived from two different types of data (table 1). The Wet Dry Line (WDL) was digitized from historical aerial photography dating from 1940 to 2015 with approximately decadal resolution. In addition, the Mean High Water (MHW) shoreline was extracted from 14 light detection and ranging (lidar) elevation surveys dating from 1998 to 2014 with approximately annual resolution (Henderson and others, 2017).

The aerial imagery (table 1) was acquired from several sources, including the U.S. Geological Survey (USGS) (https://earthexplorer.usgs.gov/), the U.S. Department of Agriculture (USDA)—Farm Service Agency (https://www.fsa.usda.gov/programs-and-services/aerial-photography/index), the University of Alabama's Cartographic Research Laboratory (http://alabamamaps.ua.edu/), and the USDA Geospatial Data Gateway (https://gdg.sc.egov.usda.gov/) as direct digital downloads or scanned images on hard disk. The image datasets from 1940, 1952, 1960, 1974, 1985, 1989, and 1997 were not assigned a coordinate system and were, therefore, georeferenced using Environmental Systems Research Institute, Inc. (Esri), ArcGIS software version 10.3.1 (http://www.esri.com/software/arcgis). Using the ArcMap Georeference toolbar, control points were established at durable structures and observable geomorphic features that remain stationary on multiple images in the dataset. The Root Mean Square error of the horizontal positions of these stationary features was used to define the uncertainty associated with georeferencing the aerial imagery. All calculations were performed using the ArcMap software. Additional sources of uncertainty accounted for in the shoreline change analysis include the natural variability in the WDL (4.5 m, for example, Pajak and Leathermann, 2002) and the uncertainty based on the cell size of each georeferenced image. Using ArcMap 10.3.1, the imagery datasets were used to delineate and digitize shorelines at the WDL along sandy beaches and vegetated shorelines.

For each of the airborne lidar surveys (table 1), a gridded surface, corrected for the bias offsets identified by Thompson and others (2017), was created from the raw point data, and the MHW shoreline along the ocean and estuarine coast of Dauphin Island (0.24 m North American

Vertical Datum of 1988 [NAVD 88]) was extracted according to USGS standards (Weber and others, 2005). The positional uncertainty of the lidar MHW shoreline was determined using the horizontal and vertical uncertainty of the published lidar data, errors associated with gridding the lidar data, and the gridded cell size. Details of the calculation and values of positional uncertainty for each shoreline can be found in Henderson and others, 2017.

Table 1. Datasets used in this study.

[See Henderson and others (2017) for full dataset and details. m, meter; Lidar, light detection and ranging; Y, yes; N, no; n/a, not applicable]

Dataset type	Date	Total uncertainty (m)	Included in 20-year analysis
Aerial image	10/27/1940	10.5	Y
Aerial image	4/29/1952	13	Y
Aerial image	11/2/1960	9.4	Y
Aerial image	12/4/1974	9.2	Y
Aerial image	6/1/1985	10.9	Y
Aerial image	9/18/1989	11.8	N
Aerial image	2/1/1992	8.4	N
Aerial image	2/11/1997	8.4	Y
Aerial image	6/23/2006	7.6	Y
Aerial image	11/12/2015	7.5	Y
Lidar	11/2/1998	4.2	n/a
Lidar	10/2/2001	2.1	n/a
Lidar	5/5/2004	3.9	n/a
Lidar	9/19/2004	4.8	n/a
Lidar	9/1/2005	3.4	n/a
Lidar	3/14/2006	3.3	n/a
Lidar	9/21/2006	2.7	n/a
Lidar	6/27/2007	3.3	n/a
Lidar	9/8/2008	4	n/a
Lidar	1/1/2010	2.8	n/a
Lidar	9/5/2012	1.8	n/a
Lidar	7/12/2013	1.6	n/a
Lidar	1/21/2014	2.2	n/a

Change in Shoreline Position and Island Width

Open-ocean and back-barrier shoreline change rates, barrier island width, and barrier island width change rates were derived from digital shoreline and transect data published by Henderson and others (2017). The full details of the methods used to detect and digitize the shoreline are found in Henderson and others (2017). These data include digitized WDL shorelines for the open ocean and back barrier that span 75 years (1940 to 2015), HWL derived from repeat lidar surveys that span 16 years (1998 to 2014), and regularly spaced cross-shore transects (342 used for open-ocean and 325 used for the back-barrier) (fig. 2). The intersections of open-ocean and

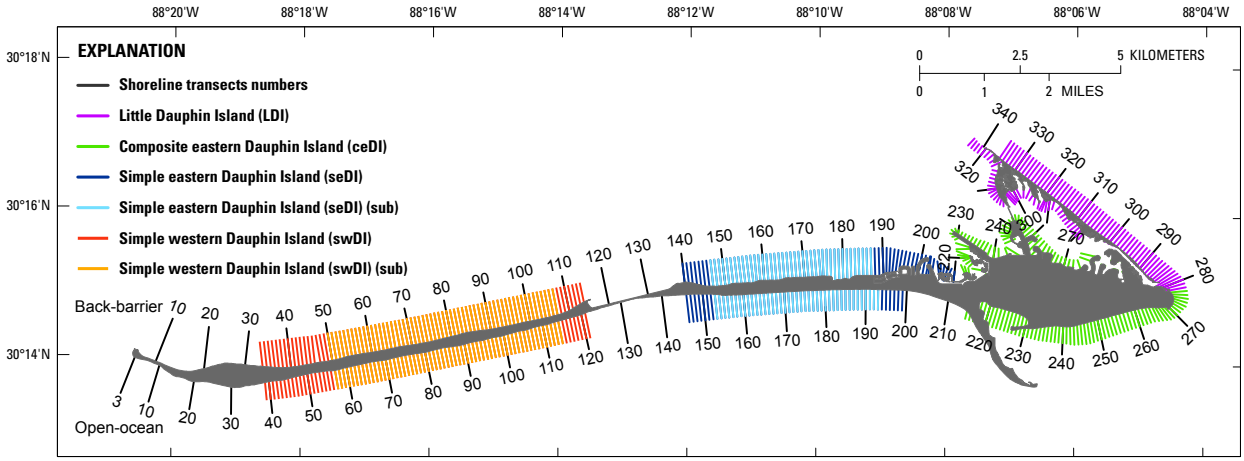

Figure 2. Map of the subaerial extent of Dauphin Island and Little Dauphin Island (see figure 1) as digitized from 2015 National Agricultural Inventory Program aerial images overlain by subset of the shoreline transects from Henderson and others (2017) used in this study to examine shoreline change rates for the four geomorphic regions of the barrier island. Two of the geomorphic regions were subsampled to further compare undeveloped and developed areas.

back-barrier shorelines (aerial and lidar) with transects were used to quantify shoreline change as Weighted Linear Regression (WLR) rate according to Thieler and others (2005). Similarly, the intersections of open-ocean and back-barrier shorelines with the transects were used to quantify island width as well as width change through time.

Prior to analysis, we divided the barrier island into four zones based on the previously mentioned geomorphic characteristics (fig. 2). These four zones (the corresponding back-barrier and open-ocean baseline transect numbers, respectively) and a brief geomorphic description are as follows:

1. swDI (32–115 and 38–122), simple barrier island section of Dauphin Island west of modern "Katrina Cut;"
2. seDI (139–211 and 145–200), simple barrier island section east of "Katrina Cut" and west of Pelican Island;
3. ceDI (212–276 and 215–277), composite barrier island section of Dauphin Island east of Pelican Island; and
4. LDI (278–325 and 278–335), Little Dauphin Island.

This binning approach provided an opportunity to compare sections with similar and dissimilar geomorphic characteristics. We also examined an additional subset of back-barrier and open-ocean transects along swDI (49–108 and 56–115, respectively) and seDI (147–188 and 153–193, respectively) to compare areas with and without infrastructure development.

Long-Term Rates

For this report, shoreline and transects provided by Henderson and others (2017) were used to extract the intersection of shoreline and transect positions, resulting in an XY position

for each date. The complete intersect dataset (date and position) was filtered to include only those transects which intersected the 1940, 2015, and three or more additional shorelines. The weighted-linear regression was computed on the subset of transects following the methodology described in Theiler and others (2005). The rates were determined using Matlab® v9.4.0.813654 (R2018a). These filtered WLR rates provide a more robust shoreline change for geomorphic comparison by excluding datasets with limited coverage and (or) not bracketing the entire 75-year period. Due to technological advancements, image resolution, and image acquisition standards, shoreline positional error in images collected in the earlier part of the 20th century is larger than those collected more recently. As such, application of the weighted-linear regression technique may favor recent over older positional data; however, by choosing image sets at similar time intervals for analysis, this potential bias may be reduced. Shoreline change rates and width change rates were averaged for the entire island, Dauphin Island, and Little Dauphin Island, and again for the four geomorphic regions.

Medium-Term Rates

The WLR method was also applied to a subset of shorelines published between 1940 and 2015 to determine change rates at approximately 20-year spacing (hereafter referred to as medium-term rates). To obtain the 20-year span (10 years between each shoreline), the following subset of shorelines was used: (1) 1940, (2) 1952, (3) 1960, (4) 1974, (5) 1985, (6) 1992, (7) 2006, and (8) 2015. Therefore, 3-point weighted-linear regression rates were produced for transects spanning the following periods: (1) 1940–1960, (2) 1952–1974, (3) 1960–1985, (4) 1974–1997, (5) 1985–2006, and (6) 1997–2015. The rates were determined using Matlab® v9.4.0.813654 (R2018a).

Short-Term Rates

The lidar-derived MHW open-ocean shorelines spanning from 1998 to 2012 (Henderson and others, 2017) were used to assess short-term rates of open-ocean shoreline change along Dauphin Island. These rates are indicative of more recent island evolution and any modern human modifications. The lidar data are used to assess this timeframe because it provides more data points (up to 14 shoreline observations) within the 16-year period than are available from aerial imagery (maximum of 3 shoreline observations). As with the digitized shorelines, data points were generated from the transect/MHW shoreline intersect points, and the data were filtered to include only those transects which intersected 1998, 2012, and three or more additional shorelines. In addition, the dataset was filtered to exclude discontinuous data (2013 and 2014). Again, the WLR rates were determined using the shoreline/transect intersect points and Matlab® v9.4.0.813654 (R2018a).

Results

Long-Term Shoreline Change (Time Step = 75 Years)

Long-term open-ocean and back-barrier shoreline change rates were determined on a subset of the transects from Henderson and others (2017). Figure 2 illustrates the transect order for each of the Dauphin Island zones, as well as the ordering of open-ocean versus back-barrier transects. Table 2 provides a summary of rates of change for open-ocean and back-barrier sites

Table 2. Summary statistics for weighted-linear regression, shoreline change rates along Dauphin Island and Little Dauphin Island.
[WLR, weighted linear regression; N, number; m y-1, meters per year; WDL, Wet Dry Line; n/m, not measured]

Open Ocean	Shoreline datasets used in analysis	Dauphin & Little Dauphin Island (Transects 37–342)			Dauphin Island (Transects 37–277)			Little Dauphin Island (Transects 278–335)		
	Year (range)	mean WLR ($m\ y^{-1}$)	sigma	N=	mean WLR ($m\ y^{-1}$)	sigma	N=	mean WLR ($m\ y^{-1}$)	sigma	N=
Long-term rates (Aerial WDL)	1940–2015	-1.80	1.62	281	-1.97	1.75	223	-1.14	0.59	58
Medium-term rates (Aerial WDL, 3-pt for 20-yr)	1940–1960	-1.33	1.89	262	-1.41	1.98	215	-0.98	1.39	47
	1952–1974	-0.91	1.62	261	-1.06	1.64	215	-0.22	1.31	46
	1960–1985	-0.86	1.53	261	-0.93	1.63	215	-0.54	0.80	46
	1974–1997	-1.06	1.92	261	-1.03	2.08	215	-1.23	0.87	46
	1985–2006	-3.26	3.41	251	-3.53	3.66	206	-2.01	1.23	45
	1997–2015	-2.94	3.36	251	-3.25	3.62	206	-1.51	0.83	45
Short-term rates (Lidar MWL)	1998–2012	n/m			-3.39	7.40	244	n/m		

Back Barrier	Shoreline datasets used in analysis	Dauphin & Little Dauphin Island (Transects 32–325)			Dauphin Island (Transects 32–277)			Little Dauphin Island (Transects 278–325)		
	Year (range)	mean WLR ($m\ y^{-1}$)	sigma	N=	mean WLR ($m\ y^{-1}$)	sigma	N=	mean WLR ($m\ y^{-1}$)	sigma	N=
Long-term rates (Aerial WDL)	1940–2015	0.06	1.09	255	0.08	1.14	217	-0.07	0.76	38
Medium-term rates (Aerial WDL, 3-pt for 20-yr)	1940–1960	0.13	3.03	244	0.15	3.25	207	-0.02	1.16	37
	1952–1974	-0.52	1.95	242	-0.59	2.00	207	-0.07	1.60	35
	1960–1985	-0.13	1.23	242	-0.21	1.25	207	0.34	1.00	35
	1974–1997	-1.39	1.38	242	-1.63	1.29	207	0.06	0.94	35
	1985–2006	0.95	2.59	229	1.16	2.68	194	-0.25	1.59	35
	1997–2015	1.77	3.62	229	2.18	3.73	194	-0.51	1.71	35
Short-term rates (Lidar MWL)	1998–2012	n/m			n/m			n/m		

assessed for the entire Dauphin Island system, Dauphin Island, and Little Dauphin Island. For open-ocean shorelines, long-term WLR rates were evaluated on 281 (of the 342) transects: 223 at Dauphin Island (DI) and 58 at Little Dauphin Island (LDI) (table 2; fig. 2). For the back-barrier shorelines, long-term WLR rates were evaluated on 255 (of the 325) transects: 217 along Dauphin Island and 38 along Little Dauphin Island.

The long-term open-ocean shoreline change rate (table 2) for the entire study area (DI and LDI) is –1.80 meters per year (m y^{-1}) with a high degree of spatial and temporal variability (standard deviation of 1.62 m y^{-1}). Means and standard deviations computed for Dauphin Island (–1.97±1.75 m y^{-1}) are slightly higher than at Little Dauphin Island (–1.14±0.59 m y^{-1}) (table 2). The mean open-ocean shoreline change rate for the geomorphic regions of Dauphin Island decreases from west (–2.53 m y^{-1}, n=85) to east (–0.38 m y^{-1}, n=59) with similar variability across the three regions (table 3), independent of which transects are used within seDI and swDI (table 4). In contrast, the average back-barrier shoreline change rate for the entire island approaches zero (0.06±1.09 m y^{-1}) with a spatial/temporal variability of 1 m y^{-1} (one standard deviation). Similarly, the mean back-barrier shoreline change rate for DI and LDI, individually, approaches zero and each has about 1 m y^{-1} of spatial/temporal variability. Unlike the open-ocean shoreline, the three regions of Dauphin Island do not exhibit an alongshore trend in back-barrier shoreline change rates (table 3; fig. 3); rather, swDI and ceDI have similar means (–0.42±0.94, n=83 and –0.20±1.07 m y^{-1}, n=43), and seDI rates are twice as high and in the opposite direction (for example, prograding) 0.65±1.14 (n=68). The same pattern and magnitude of difference between seDI and swDI was observed in the smaller transect set as well (table 4).

Medium-Term Shoreline Change (Time Step ~20 Years)

A subset of the shorelines published by Henderson and others (2017) was used to evaluate shoreline change rates at approximately a 20-year resolution (table 3; figs. 3, 4). For the entire barrier island open-ocean shoreline, the mean shoreline change rate for each of the 20-year periods examined is within the range observed for the long-term shoreline (–1.80±1.62 m y^{-1}; table 2); however, there is a notable increase in shoreline change rates when the 2006 and 2015 shorelines are included. The rates prior to inclusion of these latter shorelines are between –0.86 and –1.33 m y^{-1}; while the mean rates including the 2006 and 2015 shorelines are 1–2 m y^{-1} greater. Of the four geomorphic regions, shoreline erosion increased along swDI and seDI during the last 20 years (tables 3, 4). Prior to this period, average rates for all four regions were comparable. There is significant spatial variability within the ceDI region, but the temporal variability is quite modest. In contrast, temporal and spatial variability along LDI is low.

For the back-barrier shoreline, the 20-year averages range from –1.39 to 1.77 m y^{-1} (table 2). As with the open-ocean shorelines, the highest temporal variability of shoreline change rates occurred along seDI and swDI with the most notable changes beginning with the inclusion of the 2006 shoreline (fig. 3). Back-barrier shoreline change rates were negative (erosion) and fairly uniform across the entire island dataset prior to the inclusion of 2006. With the inclusion of the 2006 shoreline, seDI and swDI shoreline change rates shifted in a positive direction; however, there was an increase in spatial variability (figs. 3, 4; back-barrier seDI and swDI).

Short-Term Shoreline Change Rates (Lidar Shorelines, ~1-Year Resolution)

Despite the increased number of shorelines in the short-term period, the alongshore-averaged, open-ocean, short-term shoreline change rates are like those computed from aerial

Table 3. Summary statistics for weighted-linear regression, shoreline change rates along the three geomorphic regions of Dauphin Island and Little Dauphin Island.

[WLR, weighted linear regression; N, number; m y-1, meters per year; WDL, Wet Dry Line; n/m, not measured]

Open Ocean	Shoreline datasets used in analysis	Simple western Dauphin Island (Transects 37 - 122)			Simple eastern Dauphin Island (Transects 145 - 200)			Complex eastern Dauphin Island (Transects 215 - 277)			Little Dauphin Island (Transects 278 - 335)		
	Year (range)	mean WLR ($m\ y^{-1}$)	sigma	N=	mean WLR ($m\ y^{-1}$)	sigma	N=	mean WLR ($m\ y^{-1}$)	sigma	N=	mean WLR ($m\ y^{-1}$)	sigma	N=
Long-term rates (Aerial WDL)	1940–2015	-2.53	± 1.39	85	-1.67	± 0.88	56	-0.38	± 1.31	59	-1.14	± 0.59	58
Medium-term rates (Aerial WDL, 3-pt for 20-yr)	1940–1960	-2.54	± 1.37	85	-0.67	± 0.33	56	-0.50	± 2.88	59	-0.98	± 1.39	47
	1952–1974	-1.73	± 1.43	85	-0.84	± 0.37	56	-0.20	± 2.29	59	-0.22	± 1.31	46
	1960–1985	-1.65	± 0.98	85	-0.78	± 0.16	56	0.04	± 2.58	59	-0.54	± 0.80	46
	1974–1997	-1.46	± 1.33	85	-1.07	± 0.22	56	-0.17	± 3.49	59	-1.23	± 0.87	46
	1985–2006	-4.59	± 2.65	85	-3.83	± 2.25	56	-0.75	± 3.08	59	-2.01	± 1.23	45
	1997–2015	-4.24	± 2.78	85	-3.44	± 3.25	56	-0.96	± 3.37	59	-1.51	± 0.83	45
Short-term rates (Lidar MWL)	1998–2012	-5.59	± 5.18	81	-4.77	± 4.87	55	-0.81	± 4.32	60	n/m		

Back Barrier	Shoreline datasets used in analysis	Simple western Dauphin Island (Transects 32 - 115)			Simple eastern Dauphin Island (Transects 139 - 211)			Complex eastern Dauphin Island (Transects 212 - 276)			Little Dauphin Island (Transects 278 - 325)		
	Year (range)	mean WLR ($m\ y^{-1}$)	sigma	N=	mean WLR ($m\ y^{-1}$)	sigma	N=	mean WLR ($m\ y^{-1}$)	sigma	N=	mean WLR ($m\ y^{-1}$)	sigma	N=
Long-term rates (Aerial WDL)	1940–2015	-0.42	± 0.94	83	0.65	± 1.14	68	-0.20	± 1.07	43	-0.07	± 0.76	38
Medium-term rates (Aerial WDL, 3-pt for 20-yr)	1940–1960	-1.43	± 1.07	83	1.92	± 4.30	68	0.47	± 3.24	40	-0.02	± 1.16	37
	1952–1974	-1.07	± 0.86	83	-0.56	± 2.65	68	0.44	± 2.40	40	-0.07	± 1.60	35
	1960–1985	-0.92	± 0.65	83	0.46	± 1.40	68	-0.05	± 1.38	40	0.34	± 1.00	35
	1974–1997	-1.88	± 0.55	83	-1.69	± 1.43	68	-0.50	± 1.57	40	0.06	± 0.94	35
	1985–2006	1.37	± 2.15	83	1.88	± 3.18	67	-0.92	± 0.98	40	-0.25	± 1.59	35
	1997–2015	2.42	± 3.43	83	3.51	± 4.34	67	-0.63	± 0.88	40	-0.51	± 1.71	35
Short-term rates (Lidar MWL)	1998–2012	n/m			n/m			n/m			n/m		

Table 4. Weighted-linear regression, shoreline change rates computed for simple barrier island part of Dauphin Island, divided as geomorphic regions seDI and swDI, using two different clusters of transects.

[WLR, weighted linear regression; N, number; m y-1, meters per year; WDL, Wet Dry Line; n/m, not measured]

Open Ocean	Shoreline datasets used in analysis	Simple western Dauphin Island						Simple eastern Dauphin Island					
		(Transects 37–122)			(Transects 56–115)			(Transects 145–200)			(Transects 153–193)		
	Year (range)	mean WLR ($m\ y^{-1}$)	sigma	N=	mean WLR ($m\ y^{-1}$)	sigma	N=	mean WLR ($m\ y^{-1}$)	sigma	N=	mean WLR ($m\ y^{-1}$)	sigma	N=
Long-term rates	1940–2015	-2.53	± 1.39	85	-3.03	± 0.24	60	-1.67	± 0.88	56	-1.39	± 0.37	41
Medium-term rates	1940–1960	-2.54	± 1.37	85	-2.99	± 0.75	60	-0.67	± 0.33	56	-0.58	± 0.30	41
	1952–1974	-1.73	± 1.43	85	-1.99	± 0.55	60	-0.84	± 0.37	56	-0.75	± 0.28	41
	1960–1985	-1.65	± 0.98	85	-1.94	± 0.55	60	-0.78	± 0.16	56	-0.75	± 0.14	41
	1974–1997	-1.46	± 1.33	85	-2.04	± 0.36	60	-1.07	± 0.22	56	-1.03	± 0.17	41
	1985–2006	-4.59	± 2.65	85	-5.45	± 0.92	60	-3.83	± 2.25	56	-3.17	± 0.79	41
	1997–2015	-4.24	± 2.78	85	-4.79	± 1.15	60	-3.44	± 3.25	56	-2.50	± 1.50	41
Short-term rates	1998–2012	-5.59	± 5.18	81	-5.17	± 1.55	54	-4.77	± 3.47	55	-3.18	± 2.07	40

Back Barrier	Shoreline datasets used in analysis	Simple western Dauphin Island						Simple eastern Dauphin Island					
		(Transects 32–115)			(Transects 49–108)			(Transects 145–200)			(Transects 147–188)		
	Year (range)	mean WLR ($m\ y^{-1}$)	sigma	N=	mean WLR ($m\ y^{-1}$)	sigma	N=	mean WLR ($m\ y^{-1}$)	sigma	N=	mean WLR ($m\ y^{-1}$)	sigma	N=
Long-term rates	1940–2015	-0.42	± 0.94	83	-0.42	± 0.95	60	0.65	± 1.14	68	0.62	± 0.69	42
Medium-term rates	1940–1960	-1.43	± 1.07	83	-1.46	± 0.89	60	1.92	± 4.30	68	2.38	± 3.80	42
	1952–1974	-1.07	± 0.86	83	-1.03	± 0.35	60	-0.56	± 2.65	68	-1.37	± 0.87	42
	1960–1985	-0.92	± 0.65	83	-0.94	± 0.44	60	0.46	± 1.40	68	0.67	± 1.46	42
	1974–1997	-1.88	± 0.55	83	-1.99	± 0.31	60	-1.69	± 1.43	68	-2.16	± 0.80	42
	1985–2006	1.37	± 2.15	83	1.73	± 2.28	60	1.88	± 3.18	67	2.47	± 1.98	41
	1997–2015	2.42	± 3.43	83	2.36	± 2.74	60	3.51	± 4.34	67	3.54	± 1.74	41
Short-term rates	1998–2012	n/m			n/m			n/m			n/m		

imagery collected between 1997 and 2015 (tables 2, 3). The spatially averaged shoreline change rate for the entirety of Dauphin Island using the lidar-derived shorelines was –3.39 m y^{-1} with a standard deviation of 3.7 m y^{-1}. When separated into different geomorphic regions, the spatially averaged shoreline change rates and standard deviations for the transects within swDI, seDI, and ceDI are –5.59±5.18 (n=81), –4.77±4.87 (n=55), and –0.81±4.32 m y^{-1} (n=60), respectively. The standard deviation in lidar-derived shoreline change rate along the entirety of Dauphin is larger than the standard deviation computed using image-based shorelines, which may reflect

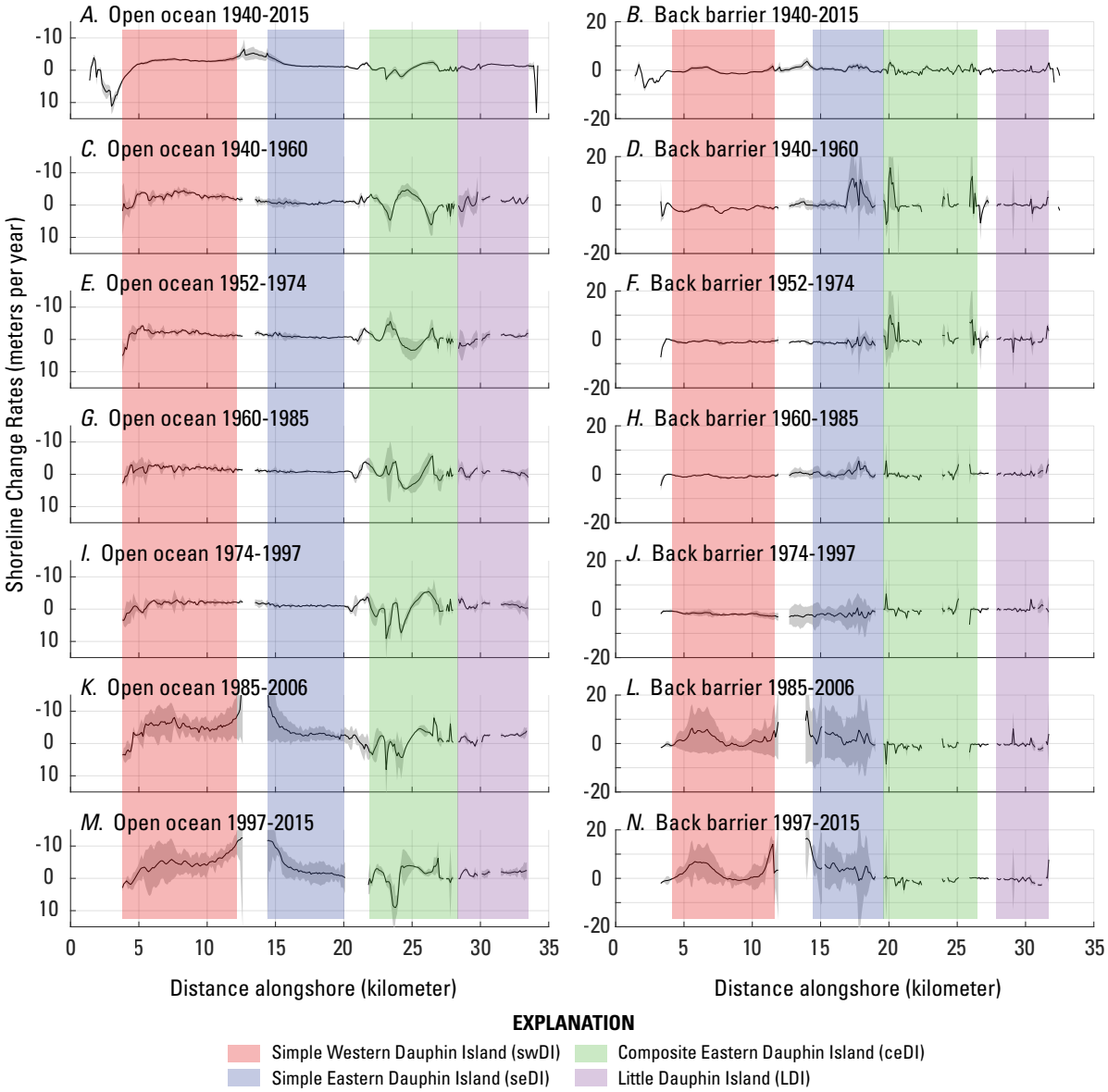

Figure 3. An assembly of weighted-linear regression, shoreline change rates (slope; solid line) and uncertainty (one sigma; shaded envelope) computed for the open-ocean (*A, C, E, G, I, K, M*) and back-barrier (*B, D, F, H, J, L, N*) shorelines for different time-periods (see table 2). The occurrence of the four major geomorphic subdivisions alongshore (west to east) follow the color code in figure 2. For both columns, northward migration (erosion of the open-ocean shoreline, progradation of the back-barrier shorelines) is toward the top of the page and vice versa.

alongshore-varying storm impacts captured by more frequent lidar surveys, some of which were sampled directly after a large storm event for damage assessments.

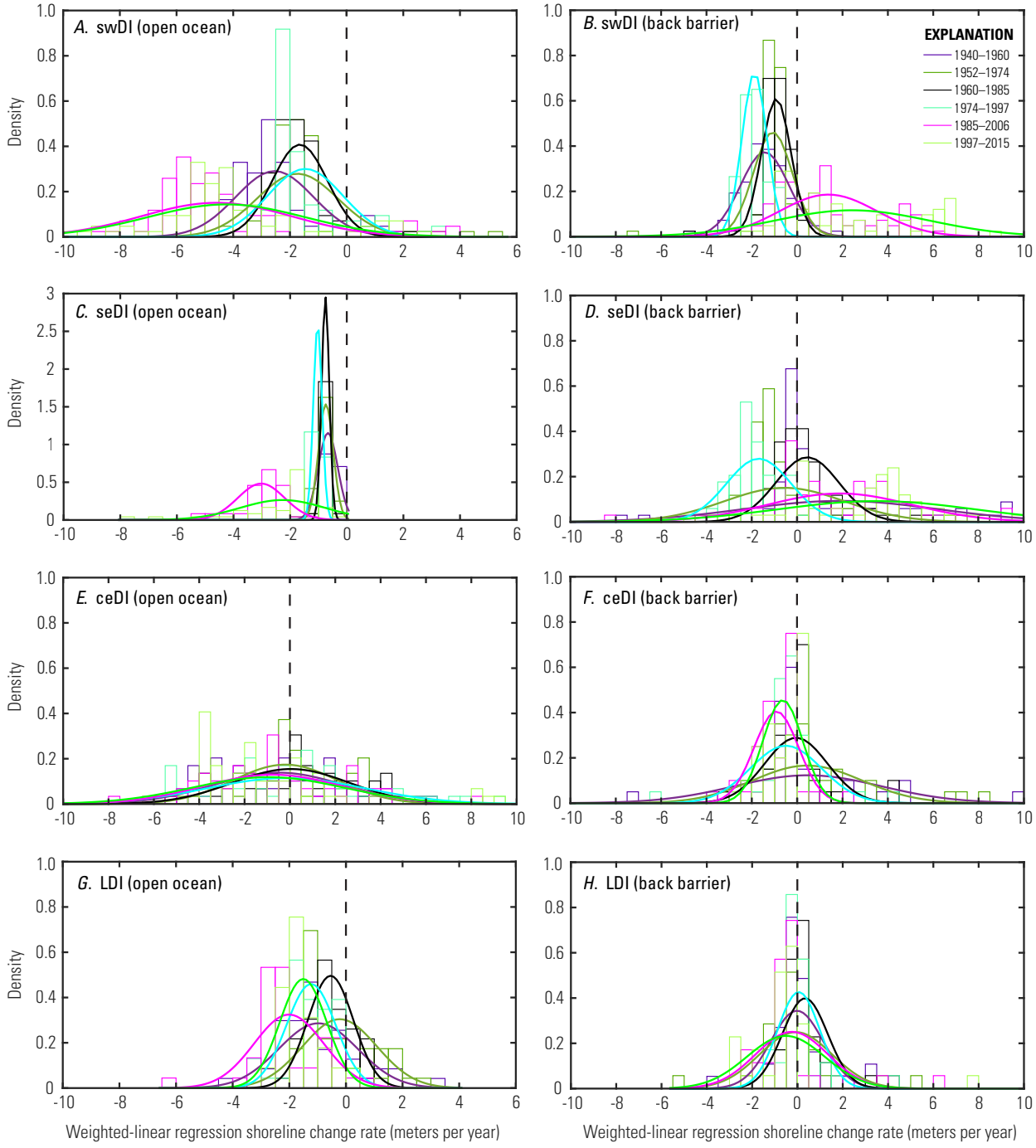

Figure 4. Density distribution of weighted-linear regression, shoreline change rates derived for the four zones on 20-year time steps (rows): (*A, B*) swDI—simple western Dauphin Island; (*C, D*) seDI—simple eastern Dauphin Island; (*E, F*) ceDI —composite eastern Dauphin Island; and (*G, H*) LDI—little Dauphin Island. The open-ocean shoreline results are presented in the left column (*A, C, E, G*), and the back-barrier results are presented in the right column (*B, D, F, H*).

Barrier Island Width

As mentioned previously, the long-term changes of swDI and seDI did not vary in magnitude or trend when fewer transects were considered (table 4). For both areas, there was persistent landward migration of the ocean shoreline yet there were different back-barrier behaviors (swDI–back-barrier shoreline loss and seDI–back-barrier shoreline gain). The effect of these contrasting patterns between swDI and seDI is apparent when comparing island width (table 5). For the swDI section, the island experienced a continual decrease in width over the 75-year period examined with a loss of 226 m of island width. Width change between consecutive WDL datasets was linear through time with no evidence of width gain. Width along seDI also decreased linearly but with width gain during the early- to mid-20th century (fig. 5). Net changes along seDI, however, were on the same order as the overall uncertainty of the measurements.

Table 5. Barrier island width computed using the open-ocean transects for the simple barrier island part of Dauphin Island, divided as geomorphic regions seDI and swDI, using two different clusters of transects.
[m, meter; N, number]

Open-ocean transects	Simple western Dauphin Island (Transects 37–122)				Simple eastern Dauphin Island (Transects 145–200)			
	Barrier island width			Change since 1940	Barrier island width			Change since 1940
Year Range	mean (m)	sigma (m)	N=	(m)	mean (m)	sigma	N=	(m)
1940	465 ±	75	85		357 ±	96	51	
1952	414 ±	56	85	-51	418 ±	65	54	61
1960	387 ±	50	85	-78	381 ±	62	56	24
1974	348 ±	49	85	-117	360 ±	59	56	3
1985	324 ±	42	85	-141	354 ±	66	56	-3
1997	275 ±	46	85	-190	276 ±	64	56	-81
2006	254 ±	42	85	-211	306 ±	96	56	-51
2015	239 ±	49	85	-226	296 ±	70	56	-61
Open-ocean transects	**Simple western Dauphin Island (Transects 56–115)**				**Simple eastern Dauphin Island (Transects 153–193)**			
	Barrier island width			Change since 1940	Barrier island width			Change since 1940
Year Range	mean (m)	sigma (m)	N=	(m)	mean (m)	sigma	N=	(m)
1940	489 ±	65	60		341 ±	83	40	
1952	429 ±	56	60	-60	405 ±	40	40	64
1960	400 ±	51	60	-89	370 ±	36	41	29
1974	359 ±	50	60	-130	353 ±	29	41	11
1985	330 ±	45	60	-159	360 ±	52	41	18
1997	271 ±	44	60	-218	276 ±	35	41	-65
2006	249 ±	23	60	-240	340 ±	39	41	-1
2015	225	33	60	-264	298	53	41	-44

Discussion

Transport Across the Barrier

A stable sediment supply is required for the formation of laterally prograding barrier islands/spits. The sediment that formed Dauphin Island originated from material stored in the Mobile Channel Pass ebb-tide delta (ETD), sediment eroded from Morgan Peninsula and bypassing the ETD, and local material eroded from outcropping Pleistocene-age surfaces of eastern Dauphin Island (Otvos, 1985). As these island types grow in length, both alongshore and cross-barrier transport become equally important in long-term stability. Two previous studies (Byrnes and others, 2010, and Morton, 2008) have documented the change in area of Dauphin Island and examined some of the impending controls (for example, lateral progradation storms and sea level). Byrnes and others (2010), using only the simple portion of Dauphin Island for calculations (our swDI and seDI), noted a net decrease of 1.34 square kilometers (km^2) between 1957 and 2006. On the other hand, Morton (2008), using the entirety of Dauphin Island, noted areal gain of about 1.29 km^2 between 1940 and 1958, followed by a net loss of 2.55 km^2 between 1958 and 2007. Despite discrepancies inherent in the two different extents used in the computations,

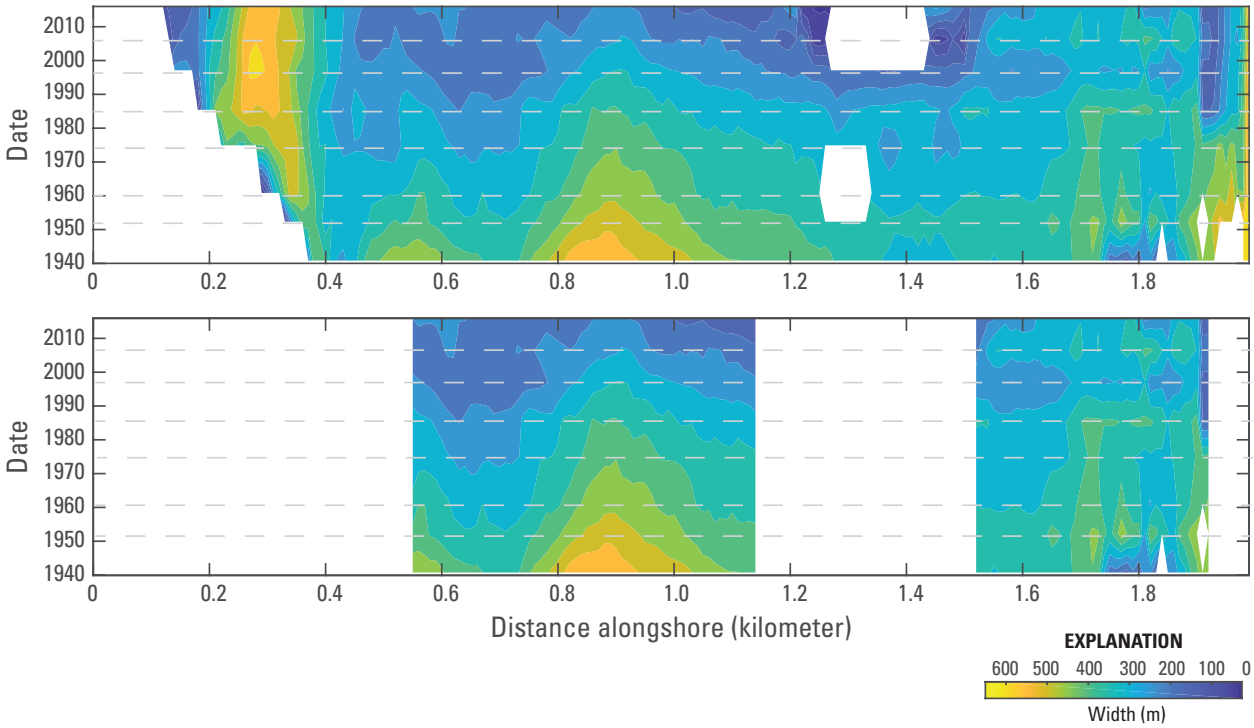

Figure 5. Contour plot showing the width of the simple portion of Dauphin Island (swDI and seDI) as it changed over the course of the study. The figure is oriented west to east with the alongshore origin corresponding to transect 1 and extending to transect 198 in figure 2. The top panel includes areas that would later be breached by Hurricanes Ivan and Katrina, and the bottom panels focus attention to sections of the island with very similar widths and geomorphology but contrasting development (left bounded unit is west of Katrina Cut and has no development; right bounded unit is east of Katrina Cut and includes portions of the Dauphin Island township). Width data along the western portion (transects 1–13, figure 2) of the top panel were excluded from panel due to dynamic behavior of spit during the period of time considered.

both studies documented decreasing island area despite commensurate lateral progradation of the western spit (Morton, 2008; Byrnes and others, 2010). The role that cross-barrier transports (that is, change in ocean and back-barrier shoreline position) play in influencing barrier island width is not well constrained by either study.

During the 75 years examined in this study, ocean shoreline erosion occurred along the entire barrier island system with the simple portion of Dauphin Island (swDI and seDI) experiencing the highest rates. Likewise, erosion appears to be the common mode for the back-barrier shoreline. However, based on the 20-year medium-term rates, ocean shoreline erosion was not at a constant magnitude and back-barrier shoreline change was not solely erosional. For example, during the period bracketed by the 1940 and 1960 shorelines, ocean shoreline erosion was high, yet, as previously noted, the area of the island reportedly increased (Morton, 2008; Byrnes and others, 2010). Although highly variable and within the uncertainty of datasets, the average back-barrier progradational signal and short-term width gain observed at seDI from 1940 to 1960 implies this section of the island achieved near stable cross-barrier dynamics. In contrast, data from the next 40–60 years depict an island that narrowed because of erosion from both shorelines. In fact, it is not until the late 1900s to early 2000s that back-barrier progradation re-emerges along swDI and seDI as an average signal. During these periods, open-ocean shoreline erosion remained two to three times greater than the back-barrier progradation. Nonetheless, these data support that cross-barrier transport remains a common component of the barrier island system, especially along the western four-fifths of Dauphin Island. Identifying where cross-barrier transport has occurred and the underlying cause are fundamental parameters needed for developing appropriate restoration and mitigation options for this barrier island.

Based on the 20-year rate data, the occurrence of cross-barrier transport on swDI and seDI is bracketed between 1986 and 2015. This period coincides with several tropical storm systems that had documented influence on the geomorphology of Dauphin Island as well as anthropogenic activity to mitigate additional future loss (for example, berm construction in 2000 and 2007). By far, Hurricanes Ivan and Katrina had the largest impact on the island (Froede, 2006; Horton and others, 2009) between 1986 and 2015. Prior to Hurricane Ivan, swDI and seDI were connected and the entire western end of the barrier island was continuous. During Hurricane Ivan (2004) storm waves and surge breached Dauphin Island, connecting Mississippi Sound with the Gulf of Mexico (Froede, 2006). In late August 2005, waves and storm surge associated with Hurricane Katrina flooded most of the island, and the small breach (60–200 m) grew to a substantial inlet (2,000 m–Katrina Cut). The inlet allowed more exchange between the Gulf of Mexico and Mississippi Sound than the previous breach, resulting in increased salinity in back-barrier bays around Dauphin Island and Mississippi Sound. Between late 2005 and late 2010/early 2011, the inlet remained open. It was during this time that the sections of the barrier island flanking the inlet (that is, spits) grew in terms of width (that is, widened). Color aerial images collected over the inlet during the 5-year period display visible shoals and sand waves on the sound side of the inlet. Trapping of alongshore sediment and the formation of recurve spits account for the positive rates of back-barrier progradation. Although our analysis excludes the inlet area proper—lack of 2015 shoreline—the flanks of the island adjacent to the inlet grew during this period. In late 2010 and as a response to potential oil movement (from the 2010 Deepwater Horizon event) into back-barrier regions of Dauphin Island, the decision to close the inlet was made and implemented with a completion date of April 2011.

Several studies have suggested that inlets play an important role in maintaining barrier island width (Kraft, 1971; Kraft and others, 1979). A recent study along the Outer Banks of North Carolina suggests that relict inlet and flood-tide delta (FTD) deposits contribute a majority of the subsurface units of the modern barrier island systems (Mallinson and others, 2010). In this setting, wider portions of the island are associated with recent migrating inlets while the narrower regions are associated with much older FTD and washover plains. Seminack and Buynevich (2013) noted that wider areas of Assateague Island, Maryland, were underlain by relict inlet and inlet-associated (recurve spit) deposits, like the findings on the Outer Banks, N.C. Dauphin Island, too, has remnants of former shallow inlets that expanded the width of the island. The land mass around Lafitte and Quivira Bays on Dauphin Island was developed between 1917 and 1934 based on maps provided in Byrnes and others (2010) and Morton (2008). Smith and others (2008) suggested that human intervention of inlet progression (for example, closure of the 1962 Buxton Inlet) between Avon and Buxton on the Outer Banks, N.C., may have curtailed natural widening processes like those observed north of the area within the Pea Island National Wildlife Refuge. Over the last 75 years, there has been very limited inlet formation along Dauphin Island. The one occurrence where breach and inlet formation allowed cross-barrier transport followed Hurricane Katrina (August 2005), but due to unnatural and unique pressures (DWH oil migration), the inlet had to be closed with only 6 years (completion April 2011) of exchange between the Gulf of Mexico and Mississippi Sound.

Overwash is also an important mechanism for cross-barrier transport. Time-series aerial imagery provide evidence of widespread overwash along seDI, swDI, and LDI at multiple times throughout Dauphin Island's history. Between 1992 and 2006, cumulative overwash from multiple storms (mostly Hurricanes Ivan and Katrina) is present as a sandy surface, occupying formerly vegetated surfaces as well as municipal and residential features (lawns, driveways, roads, and so forth). During the period between 1997 and 2006, swDI appears to have decreased in width by only a minor amount or had no change in width at all; however, the barrier footprint migrated northward a few tens of meters. Similar, seDI migrated northward during this time with a similar magnitude, but the area gained approximately 50 m of barrier island width. Again, this width change is observed in the means of the western Dauphin Island mean width versus time (table 5). Subsequently from 2006 to 2015, erosion on both the back-barrier and open-ocean shorelines has reduced the gain from earlier periods. Using this decadal analysis, the frequency of overwash due to minor and major storms is not addressed. Since imagery is just singular points in time, modeling of multiple storms in closely space time periods may help address why some areas gained land following storms and others did not. It can be assessed that overwash, even in developed regions, can aid in gaining barrier island width through the deposition of washover fans. Post-depositional modification to these washover fans (mining sand, artificial movement of sand to foredunes, and so forth) affects the island's ability to migrate northward.

Modifications Along Back-Barrier Environments

Vegetated areas (namely shrub/scrub uplands and marshes) are important environments on barrier island systems that serve as critical habitat for numerous species of birds, fish, reptiles, and amphibians (Enwright and others, 2017). These environments are also important to the physical evolution of barrier islands by increasing back-barrier elevation through vertical accumulation of organic and inorganic sediment, trapping aeolian and washover sediments, and often stabilizing shoreline with cohesive sediments (Deaton and others, 2017). Vegetated areas on Dauphin Island were more abundant prior to the development of the island (Byrnes and others,

2010). Today, marsh environments are isolated to LDI and a small marsh platform located in Graveline Bay behind ceDI (Enwright and others, 2017). The back-barrier regions of LDI (including Cedar Island) have remained fairly constant in shape and size during the past 75 years, whereas the back-barrier region where modern Graveline Bay marshes exist has changed morphology and size significantly during this period. Ellis and other (2018) found that sediment data from both LDI and Graveline Bay regions indicate marsh environments and those environments have been accreting vertically at rates (3.73±2.71 millimeters per year, mm y^{-1}) comparable to sea-level rise for the region. This would suggest that elevation gain by sediment trapping and organic matter accumulation may be influencing wetland loss but, given uncertainty in rates, it probably is not the primary cause. One of the biggest losses of wetland area can be attributed directly to human modification. Between 1952 and 1960, a large marsh platform wedged between the back-barrier regions of LDI and ceDI was exhumed and filled for development of residential communities and boat access. Graveline Bay marshes were generally left in tack except for the formation of a navigation channel cut between the marsh platform and the island and the construction of the Dauphin Island runway. Erosion rates (~1.0 m y^{-1}) along the Graveline Bay marsh shoreline are an order of magnitude greater than the average back-barrier erosion for the entire Dauphin Island (0.2 m y^{-1}). Thus, erosion dominates marsh loss in Graveline Bay.

Change in vegetated areas of Dauphin Island is one area of uncertainty that may have influenced the stability of the island. By analogy of island and vegetated surface, LDI is by far more diverse and has less vegetated environments. In LDI, many washover fans that cross the island are stabilized by vegetation and ensure elevation and any width gain are sustained by reducing winnowing from winds. Thus, LDI may serve as a reasonable generic model for the distribution of back-barrier vegetated environments (based on width and elevation) for any potential restoration scenarios on Dauphin Island. The complicating factor is that the two islands are exposed to different wave energy regimes and thus should be evaluated with proper observation and combined physical and ecological modeling. Unlike Dauphin Island which is exposed to the waves in the Gulf of Mexico, the Little Dauphin Island shoreline is only exposed to Mobile Bay, which has lower energy and shorter period waves associated with the limited fetch available for wave generation.

Summary

Over the last 75 years, Dauphin Island and Little Dauphin Island have experienced erosion of both the open-ocean and back-barrier shorelines, which has caused the width of the islands to decrease. Previous studies have attributed this land loss to reduced littoral sediment budgets associated with historical anthropogenic activities around Dauphin Island and Mobile Bay. Our imagery analysis does not provide the information needed to fully link shoreline change with volumetric gains or losses of island sediment. The data do, however, provide a clear indication that cross-barrier transport, which is also critical to the maintenance of the island, has been limited. Specifically, the formation of Katrina Cut was one of the first inlets to form along western Dauphin Island since the early 1900s. In other barrier island systems, inlets have shown to significantly aid in the development and maintenance of barrier island width-enabling transgression. It is uncertain whether Katrina Cut may have benefited the islands through growth in area as the inlet was managed within 6 years of opening to reduce the threat of oil migration into critical habitats around Dauphin Island. There is evidence that overwash has temporally contributed to back-barrier progradation but long-term stabilization of such features by vegetation is only observed on the area west of Katrina Cut. Overall, the disequilibrium between oceanic shoreline erosion and back-barrier progradation remains an important management decision

that needs to be addressed. Unfortunately, the trend in width change has been constant for much of the past 75 years. Whether this is a normal response for Dauphin Island or a response to additional pressure from external drivers (humans, sea level, hurricanes) remains uncertain. Additional modeling experiments that allow for perturbations evaluated over a 10+ year duration, which is an objective of the Alabama Barrier Island Study, may provide insight to these uncertainties.

References Cited

Byrnes, M.R., Griffee, S.F., and Osler, M.S., 2010, Channel dredging on geomorphic response at and adjacent to Mobile Pass, Alabama: Vicksburg, Miss., U.S. Army Corps of Engineers Research and Development Center, Coastal and Hydraulics Laboratory, ERDC/CHL TR-10-8, 309 p., accessed March 2, 2018, at http://www.dtic.mil/docs/citations/ADA536622.

Deaton, C.D., Hein, C.J., and Kirwan, M.L., 2017, Barrier island migration dominates ecogeomorphic feedbacks and drives salt marsh loss along the Virginia Atlantic Coast, U.S.A.: Geology, v. 45, no. 2, p. 123–126, accessed March 2, 2018, at https://doi.org/10.1130/G38459.1.

Douglas, S.L., 1994, Beach erosion and deposition on Dauphin Island, Alabama, U.S.A.: Journal of Coastal Research, v. 10, no. 2, p. 306–328, accessed March 27, 2014, at https://www.jstor.org/stable/4298218.

Ellis, A.M., Smith, C.G., and Marot, M.E., 2018, The sedimentological characteristics and geochronology of the marshes of Dauphin Island, Alabama: U.S. Geological Survey Open-File Report 2017–1165, accessed May 2, 2018, at https://doi.org/10.3133/ofr20171165.

Enwright, N.M., Borchert, S.M., Day, R.H., Feher, L.C., Osland, M.J., Wang, L., and Wang, H., 2017, Barrier island habitat map and vegetation survey—Dauphin Island, Alabama, 2015: U.S. Geological Survey Open-File Report 2017–1083, 17 p., accessed May 2, 2018, at https://doi.org/10.3133/ofr20171083.

Froede, C.R., Jr., 2006, The impact that Hurricane Ivan (September 16, 2004) made across Dauphin Island, Alabama: Journal of Coastal Research, v. 22, no. 3, p. 561–573, accessed May 2, 2018, at https://doi.org/10.2112/05-0438.1.

Henderson, R.E., Nelson, P.R., Long, J.W., and Smith, C.G., 2017, Vector shorelines and associated shoreline change rates derived from lidar and aerial imagery for Dauphin Island, Alabama—1940–2015: U.S. Geological Survey data release, accessed May 2, 2018, at https://doi.org/10.5066/F7T43RB5.

Horton, B.P., Rossi, V., and Hawkes, A.D., 2009, The sedimentary record of the 2005 hurricane season from the Mississippi and Alabama coastlines: Quaternary International, v. 195, no. 1, p. 15–30, accessed November 22, 2015, at https://doi.org/10.1016/j.quaint.2008.03.004.

Hummell, R.L., 1999, Geologic and economic characterization and near-term potential of sand resources of the east Alabama inner continental shelf offshore of Morgan Peninsula Alabama: Geological Survey of Alabama, final report, 231 p.

Kraft, J.C., 1971, Sedimentary facies patterns and geologic history of a Holocene marine transgression: Geological Society of America Bulletin, v. 82, no. 8, p. 2131–2158, accessed March 2, 2018, at https://doi.org/10.1130/0016-7606(1971)82[2131:SFPAGH]2.0.CO;2.

Kraft, J.C., Allen, E.A., Belknap, D.F., John, C.J., and Maurmeyer, E.M., 1979, Processes and morphologic evolution of an estuarine and coastal barrier system, *in* Leatherman, S.P., ed., Barrier islands from the Gulf of St. Lawrence to the Gulf of Mexico: New York, Academic Press, p. 149–184.

Mallinson, D.J., Smith, C.W., Culver, S.J., Riggs, S.R., and Ames, D., 2010, Geological characteristics and spatial distribution of paleo-inlet channels beneath the outer banks barrier islands, North Carolina, U.S.A.: Estuarine, Coastal and Shelf Science, v. 88, no. 2, p. 175–189, accessed January 4, 2013, at https://doi.org/10.1016/j.ecss.2010.03.024.

Morton, R.A., 2008, Historical changes in the Mississippi-Alabama barrier-island chain and the roles of extreme storms, sea level, and human activities: Journal of Coastal Research, v. 24, no. 6, p. 1587–1600, accessed January 4, 2013, at https://www.jstor.org/stable/40065143.

Otvos, E.G., 1981, Barrier island formation through nearshore aggradation—Stratigraphic and field evidence: Marine Geology, v. 43, nos. 3–4, p. 195–243, accessed January 4, 2013, at https://doi.org/10.1016/0025-3227(81)90181-X.

Otvos, E.G., 1985, Barrier platforms—Northern Gulf of Mexico: Marine Geology, v. 63, nos. 1–4, p. 285–305, accessed January 4, 2013, at https://doi.org/10.1016/0025-3227(85)90087-8.

Otvos, E.G., Jr., 1970, Development and migration of barrier islands, northern Gulf of Mexico: Geological Society of America Bulletin, v. 81, no. 1, p. 241–246, accessed January 4, 2013, at https://doi.org/10.1130/0016-7606(1970)81[241:DAMOBI]2.0.CO;2.

Otvos, E.G., and Carter, G.A., 2008, Hurricane degradation—Barrier development cycles, northeastern Gulf of Mexico—Landform evolution and island chain history: Journal of Coastal Research, v. 24, no. 2, p. 463–478, accessed January 4, 2013, at https://doi.org/10.2112/06-0820.1.

Pajak, M.J., and Leatherman, S., 2002, The high water line as shoreline indicator: Journal of Coastal Research, v. 18, no. 2, p. 329–337, accessed 2-May-2018, at https://www.jstor.org/stable/4299078.

Riggs, S.R., Cleary, W.J., and Snyder, S.W., 1995, Influence of inherited geologic framework on barrier shoreface morphology and dynamics: Marine Geology, v. 126, nos. 1–4, p. 213–234, accessed May 4, 2018, at https://doi.org/10.1016/0025-3227(95)00079-E.

Seminack, C.T., and Buynevich, I.V., 2013, Sedimentological and geophysical signatures of a relict tidal inlet complex along a wave-dominated barrier: Assateague Island, Maryland, U.S.A.: Journal of Sedimentary Research, v. 83, no. 2, p. 132–144, accessed March 2, 2018, at https://doi.org/10.2110/jsr.2013.10.

Smith, C.G., Culver, S.J., Riggs, S.R., Ames, D., Corbett, D.R., and Mallinson, D., 2008, Geospatial analysis of barrier island width of two segments of the Outer Banks, North Carolina, U.S.A.—Anthropogenic curtailment of natural self-sustaining processes: Journal of Coastal Research, v. 24, no. 1, p. 70–83, accessed February 24, 2014, at https://www.jstor.org/stable/30134236.

Thieler, E.R., Himmelstoss, E.A., Zichichi, J.L., and Miller, T.L., 2005, The Digital Shoreline Analysis System (DSAS) version 3.0, an ArcGIS© extension for calculating historic shoreline change: U.S. Geological Survey Open-File Report 2005–1304, accessed March 2, 2018, at https://doi.org/10.3133/ofr20051304.

Thompson, D.M., Dalyander, P.S., Long, J.W., and Plant, N.G., 2017, Correction of elevation offsets in multiple co-located lidar datasets: U.S. Geological Survey Open-File Report 2017–1031, 15 p., accessed May 2, 2018, at https://doi.org/10.3133/ofr20171031.

Weber, K.M., List, J.H., and Morgan, K.L.M., 2005, An operational mean high water datum for determination of shoreline position from topographic lidar data: U.S. Geological Survey Open-File Report 2017–1031, 15 p., accessed May 2, 2018, at https://doi.org/10.3133/ofr20051027.

ISSN 2331-1258 (online)
https://doi.org/10.3133/ofr20181170